processes

MDPI

Article

Enabling Total Process Digital Twin in Sugar Refining through the Integration of Secondary Crystallization Influences

Florian Lukas Vetter and Jochen Strube *

Institute for Separation and Process Technology, Clausthal University of Technology, Leibnizstr. 15, 38678 Clausthal-Zellerfeld, Germany; vetter@itv.tu-clausthal.de
* Correspondence: strube@itv.tu-clausthal.de; Tel.: +49-5323-72-2872

Abstract: Crystallization is the main thermal process resulting in the formation of solid products and, therefore, is widely spread in all kinds of industries, from fine chemicals to foods and drugs. For these high-performance products, a quality by design (QbD) approach is applied to maintain high product purity and steady product parameters. In this QbD-context, especially demanded in the foods and drugs industry, the significance of models to deepen process understanding and moving toward automated operation is steadily rising. To reach these aspired goals, besides major process influences like crystallization temperature, other impacting parameters have to be evaluated and a model describing these influences is sought-after. In this work, the suitability of a population balance-based physico-chemical process model for the production of sugar is investigated. A model overview is given and the resulting model is compared to a statistical DoE scheme. The resulting process model is able to picture the effects of secondary process parameters, alongside temperature or temperature gradients, the influences of seed crystal size and amount, stirrer speed, and additives.

Keywords: quality by design; crystallization; sugar; foods and drugs; digital twin; modeling; DoE; natural resources

Citation: Vetter, F.L.; Strube, J. Enabling Total Process Digital Twin in Sugar Refining through the Integration of Secondary Crystallization Influences. *Processes* **2022**, *10*, 373. https://doi.org/10.3390/pr10020373

Academic Editor: Pei Liu

Received: 12 January 2022
Accepted: 11 February 2022
Published: 15 February 2022

1. Introduction

Crystallization, as a process, plays a major role in the purification and formulation of most pharmaceutical products and the food and nutrition sector [1]. Its importance in purification mainly results from the formation of pure crystals from mixed solutions [1] and thas been used in the production of sugar for centuries [2].

There are two different production processes for sucrose, based on the crops sugar cane and sugar beets [2]. These processes, however, differ mainly in the extraction and initial purification steps, e.g., the lime treatment in the production of beet sugar. Crystallization, on the other hand, is the basis for purification and formulation in both processes [2].

The main cost driver in the production of sugar is the solid–liquid separation of sugar crystals from the mother liquor. This is the reason why, in the context of automation, major advances were made in modeling and optimization of centrifugal processes [3–5]. As one of the main influences on the results and economics of a centrifugal process is particle size and particle size distribution, it is an important quality attribute of sugar crystals [6]. Hence, in combination with centrifugation a deepened process understanding of the crystallization process is needed to evaluate a total process optimum.

To answer the increased demand for high-purity natural products, resulting from changing patterns of consumption in developing countries, as well as the demand for medicines of natural origin, it is called for an efficient total process design based on a quality-by-design approach [7,8]. For the production of sugar, the potential for optimization of extraction processes via a digital twin and the resulting increased process understanding has already been shown [9]. Furthermore, other process steps in the production of sugar have sophisticated process models [3–5,10]. An overview of the potential total process modeling is given in Figure 1. Process models for the extraction of sugar from beets have been shown

to accurately model the hydrodynamic and substance transfer in the extraction process, as shown by Both et al. [9]. Furthermore, evaporation and centrifugal modeling were recently discussed in the ISJ World Sugar Yearbook by Foxon and Lehnberger, respectively [11,12]. This work shows a model-based approach to link the evaporation and centrifugal models with a sophisticated crystallization model.

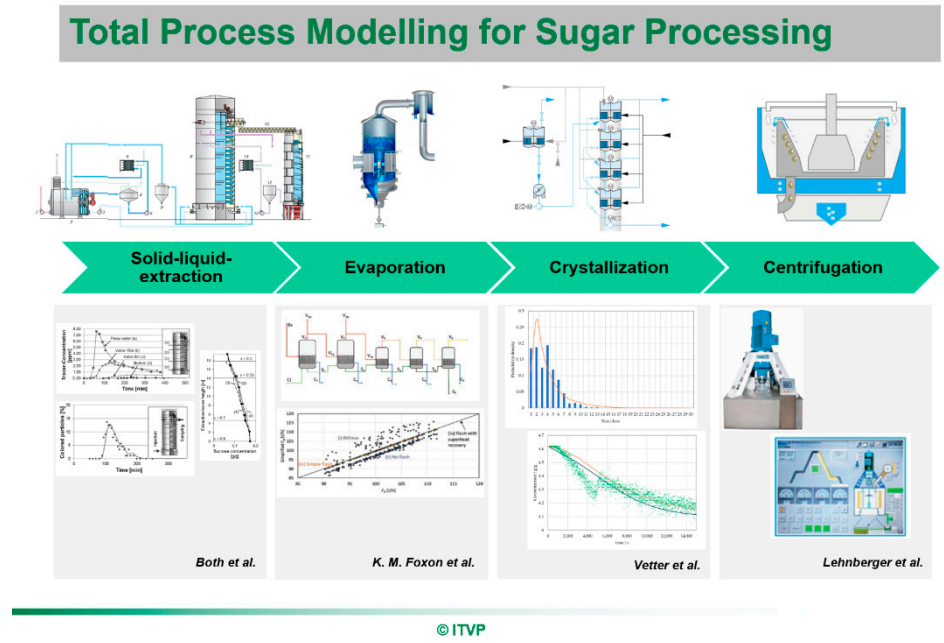

Figure 1. Visualization for the total process modeling the sugar production process.

For crystallization in general, modeling crystal growth and thereby crystallization end times dependent on the main influence—temperature—has widely been successful [13–18] in some cases also including agglomeration or crystal attrition. Other factors, however, such as seed crystal size, amount, or the addition of additives such as esters are likely to influence an industrial sucrose process [2].

The aim of this paper is to propose a validated physio-chemical process model as digital twin, which is able to evaluate the different influences of these factors and lead to a deepened process understanding. Validation was achieved through the comparison with the Design of Experiments (DoE) scheme, as suggested in the literature [19,20]. Additionally, this model is compared to a statistical DoE to highlight the advantages of this method.

2. Materials and Methods

2.1. Materials

Store-bought sucrose was used in the crystallization experiments. For seed crystals, sucrose was ground with a Grindomix® 200 knife mill (Retsch GmbH, Haan, Germany). After grinding, the seed crystals were sieved into three size classes (50–100 µm, 100–150 µm, and 150–250 µm). Water was used as ultra-pure water (arium® pro, Sartorius AG, Göttingen, Germany). To suspend the seed crystals, isopropanol was used (EMSURE®, Merck KGaA, Darmstadt, Germany). As a crystallization additive, we used Esterin A 08 (EHG Ingredients, Kiev, Ukraine).

2.2. Size Distribution

The crystal sizes were measured using the Axiolab A (Zeiss, Oberkochen, Germany) light microscope. The ferret max was used as the characteristic crystal size. q_3 distributions were calculated from the q_0 distributions obtained via microscopy. The q_0 distribution

indicates the number of crystals in each size class, while the q_3 distribution indicates the crystal mass or volume found in each size class and can be calculated using Equation (1).

$$q_3(x) = \frac{x^3 q_0(x)}{\int_{x_{min}}^{x_{max}} x^3 q_0(x) dx} \quad (1)$$

To evaluate the effects on particle size and particle size distribution, a method to simplify the description of the particle size distribution was needed. A simple method to quantify these parameters is the evaluation of the measured q_0 and q_3 distributions as a RRSB (Rosin, Rammler, Sperling, and Bennet) distribution, also known as Weibull distribution, which is widely used in mechanical process engineering to describe particle size distributions [21]. Equation (2) allows obtaining d' as the reciprocal grain size parameter of the 63rd—percentile and the form parameter k from the measured probability in the size class x_1 to x_2 [21,22]. The form parameter k typically varies between 0 and 5, where 0 is a maximum skewed distribution and values over 3.5 give distributions of vanishing skewness close to a normal distribution.

$$q(x_1, x_2) = {d'}^{-k} x_2^{-k} e^{-{d'}^{-k} x_2^{-k}} \left(d' x_2\right)^k - {d'}^{-k} x_1^{-k} e^{-{d'}^{-k} x_1^{-k}} \left(d' x_1\right)^k \quad (2)$$

This method of simplifying the particle size distribution into the parameter k enables the evaluation via DoE; this also leads to the circumstance that the results of the DoE are not as easily comparable to the results of the mass balance.

2.3. Crystallization

Crystallization was conducted in a 1 L stirred double jacketed vessel, during which crystallization turbidity and temperature was measured using an EXcell 230 (Exner, Recklinghausen, Germany) turbidity sensor and a PT-100 thermometer. The crystallization vessel was stirred using a ViskoPakt®-rheo 110 (HiTec Zang, Herzogenrath, Germany) stirrer in combination with a four-blade axial flow polytetrafluoroethylene stirrer, also known as a paddler. During crystallization temperature, turbidity, torque, and RPM were recorded.

For the crystallization experiments, 800 g sugar were solved in 200 g (sic) of water at 90 °C, after turbidity reaches zero supersaturation is achieved by evaporating 56 g water. The evaporated water was condensed and caught in a weighted beaker to monitor the supersaturation. After each crystallization, crystals were analyzed in suspension using the microscope.

Crystallization end time is difficult to measure reproducibly. To get around this problem in this study, we defined the crystallization to be finished, when 95% of the final turbidity was reached. To find this value and, therefore, find the crystallization end time, we fitted a sigmoid function to the turbidity curve.

2.4. Design of Experiments (DoE)

Based on the generally acknowledged quality-by-design (QbD) approach, firstly, critical quality attributes (CQA) have to be defined to determine the impact of different process parameters on these attributes [19,23]. As the sugar crystals need to be narrowly distributed, the large crystals were decided on by these CQAs, as discussed previously. We also added crystallization time, as an economically important attribute for the crystallization process. Probable influences on the CQAs were commonly identified using an Ishikawa diagram. A general Ishikawa diagram for the crystallization process is given in Figure 2. For the design of our model, we decided on excluding "equipment" and "material" effects since sugar crystallization is an established process and sugar has excellent solubility in water, allowing for an economical process design. For the process parameters, we decided to exclude the temperature influence in our DoE; in the model, however, a temperature influence could be easily be integrated via the crystallization growth speed and sugar solubility discussed in Section 2.5.

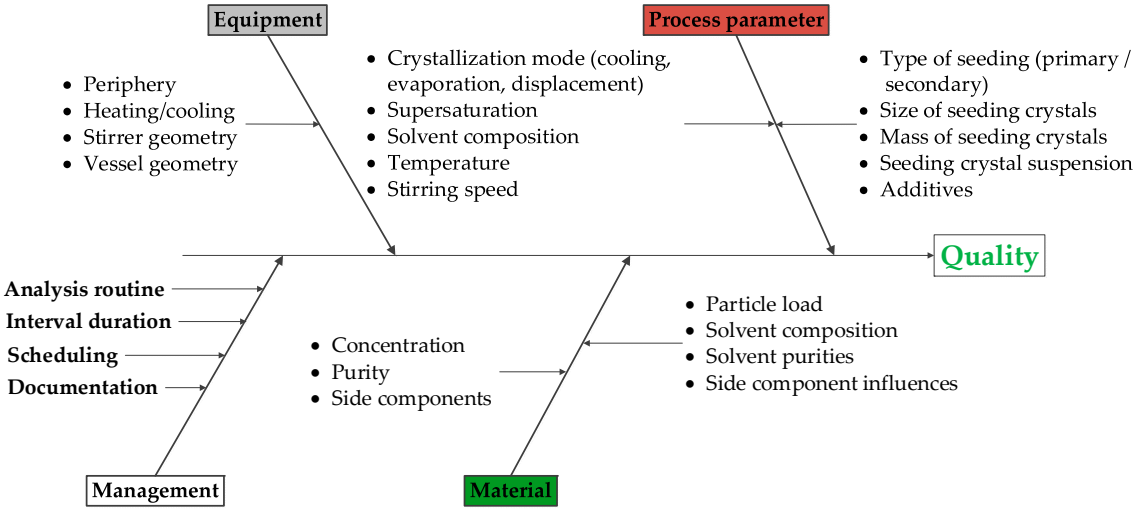

Figure 2. General Ishikawa diagram for a crystallization process.

This results in the process parameters of stirring speed, seeding crystal size, mass, and additives for our DoE. These variables were changed in a three-step, full-factorial DoE scheme. The center point was repeated three times.

Seeding crystal size was varied in the aforementioned sieving classes and the seeding crystal amount was varied in 100 mg, 200 mg, and 300 mg. Stirring speed was varied in three steps 100 rpm, 200 rpm, and 300 rpm, and the additive amount was varied in 0 mL, 1 mL, and 2 mL steps.

2.5. Modeling of Crystallization

Crystallization was modeled using a population balance model, modeling crystal growth, agglomeration, and aggregation as described in the literature [13,15,16,24] written in Equation (3). Crystal nucleation was neglected. As seeding crystals were used, secondary nucleation is the dominant mode to be expected [25].

$$\frac{\partial n}{\partial t} = \frac{\partial G n}{\partial L} - D(L) + B(L) \tag{3}$$

This balance describes the change of the number density n over time, which results from the growth rate of a single crystal G, the crystal death rate D and the crystal birth rate B for crystals of a size L. The crystal growth rate is given by Equation (4). Since the observed experimental space temperature is kept constant, this equation is simplified to (5) [13,24].

$$G = k_1 \cdot e^{-\frac{k_2}{T}} * S^{k_3} \tag{4}$$

$$G = k_{12} \cdot S^{k_3} \tag{5}$$

k_{12} and k_3 are the kinetic constants of crystal growth. S is the supersaturation defined in Equation (6) [13,24], with the sugar concentration in equilibrium c_{eq} which is given by Equation (7) [2] and is correlated from A_{eq} and B_{eq} which are determined to be $A_{eq} = 0.0857$ and $B_{eq} = 0.0106$ to give equilibrium concentration in $\frac{kg_{sucrose}}{kg_{water}}$ based on literature data [2].

$$S = \frac{c - c_{eq}}{c_{eq}} \tag{6}$$

$$c_{eq} = A_{eq} * e^{B_{eq} * T} \tag{7}$$

The change in concentration in solution is expressed with Equation (8) [17] where k_v is the shape factor, σ_S the crystal density, m_L the mass of water and L the characteristic length of the crystal. The shape factor is assumed to be $k_v = 0.87\frac{\pi}{6}$ based on literature [26].

$$\frac{\partial c}{\partial t} = -3 * \sigma_s * \frac{k_v}{m_L} * G * \int_0^\infty L^2 n \, dL \tag{8}$$

The birth and death terms in the population balance result from the effects of agglomeration and attrition. Agglomeration can be modeled with different stochastic approaches [13,16]. The birth and death terms resulting from agglomeration are given in Equation (9) and Equation (10) [13].

$$B_A = \frac{L^2}{2} \int_0^L \frac{\beta\left(\left(L^3 - \lambda^3\right)^{\frac{1}{3}}, \lambda\right) n\left(\left(L^3 - \lambda^3\right)^{\frac{1}{3}}\right) n(\lambda)}{\left(L^3 - \lambda^3\right)^{\frac{2}{3}}} d\lambda \tag{9}$$

$$D_A = n(L) \int_0^\infty \beta(L, \lambda) n(\lambda) d\lambda \tag{10}$$

These equations describe the agglomeration between two crystals with the sizes L and λ. The two-dimensional matrix $\beta(L, \lambda)$ describes the number of collisions per time for two crystals of the aforementioned sizes and is modeled as a triangle matrix according to Equation (11) [13].

$$\beta(L, \lambda) = \frac{1}{W_{eff}} \frac{2kT}{3\eta_L} (\lambda + L)\left(\frac{1}{\lambda} + \frac{1}{L}\right) \tag{11}$$

In Equation (11) W_{eff} describes the agglomeration efficiency, which can be correlated for submicron particles according to Stokes–Einstein as the collision efficiency [16]. Since the observed crystals in this work are not submicron, W_{eff} is determined using the obtained experimental data. k is the Boltzmann constant and η_L the viscosity of the solution. For highly concentrated sugar solution correlations for the viscosity are available [2].

The birth and death terms resulting from the effects of attrition are modeled based on different approaches. Either it is assumed that two different size crystals are birthed from an attrition process or more than two same size crystals are birthed from it [16,27]. In this work, it is assumed that three same-size crystals result from attrition as this best describes the experimental data. To model attrition, Equations (12) and (13) are used.

$$B_B(L) = w \, D_B(L) \tag{12}$$

$$D_B(L) = r_{Br} n(L) \tag{13}$$

In these, w is the number of crystals obtained from the attrition process and r_{Br} is the breakage rate calculated according to Equation (14) with γ and Λ being breakage constants and $\overline{E}$ being the specific energy input through stirring, calculated from the torque and rpm measured in the experiments;

$$r_{Br} = \gamma \overline{E}^{\Lambda} \tag{14}$$

2.6. Parameter Determination and Model Solution

To solve the differential equation system described in 2.5, we used Aspen Custom Modeler V 11 (Aspen Technology Inc., Bedford, MA, USA). Discretization was done according to a 1st-order backward finite difference method. We used a mixed Newton nonlinear solver and the gear integrator with a variable step size.

Most parameters are measured in the experiments or taken from literature data, as described above. There are however k_{12}, k_3, L and W_{eff}, which are determined using a NL2SOL least squares solver on the experimental data. NL2SOL is a least squares nonlinear solver employing a variation on Newton's method. For the identification, we

used least-squares as the optimization function. To identify the expected range, we used an unrestrained Nelder–Mead method and then decided on the limits given in Table 1.

Table 1. Limits used in the parameter determination.

Parameter	Lower Limit	Upper Limit
k_{12}	1×10^{-37}	1×10^{-4}
k_3	1×10^{-37}	1×10^{-4}
L	0.5	2
W_{eff}	1×10^{-37}	1×10^{37}

As training data, the concentration course was given for ten equidistant time points. The particle size was given as the measured q_0 distributions from the microscopic measurements.

3. Results

3.1. Design of Experiments

In Figure 3, examples for the experimental results are given. In (a), a very skewed distribution can be observed. This is represented by the above-mentioned parameter k giving a value of 3.22. The x_{63} is 866 µm. In comparison, (b) shows a very even distribution around 1308 µm with a form factor of 5.38. For the evaluation of each experiment, 300 crystals were evaluated. To better the understanding for these arbitrary metrics, we gave the corresponding Weibull distributions in (d–f). Particles above 1500 µm were not observed, hence, the graph is shortened.

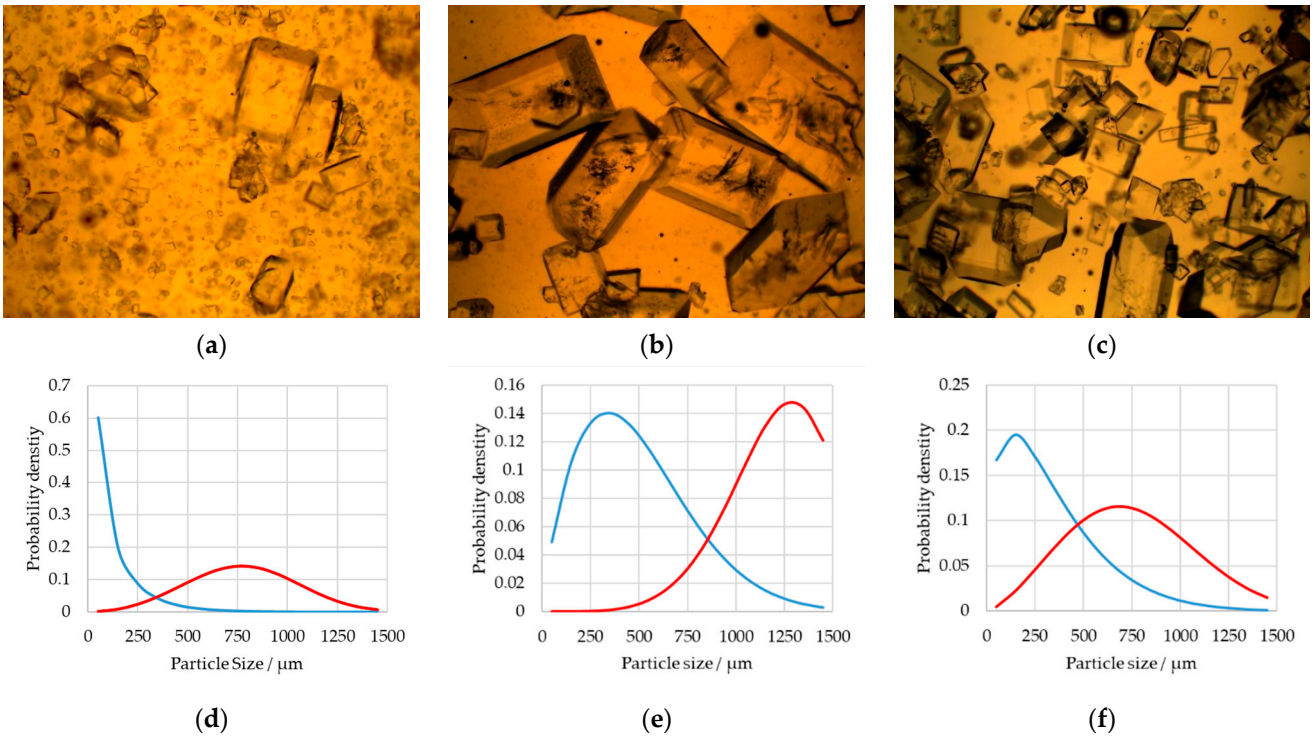

Figure 3. Crystallization results of three experiments in the DoE (**a**–**c**). In (**d**–**f**), the corresponding particle size densities are given. Here, the blue line is the q_0 distribution, and the red is the q_3 distribution.

For this process, the DoE yields some satisfying results depicted in Figure 4. The prediction for the particle size distribution, given in (b), shows a good correlation of the observed effects to the input parameters with an R^2 of 0.97 and a p-value of 0.0041. For the particle size (x_{63}) shown in (a) the prediction is not as good, while remaining statistically significant with an R^2 of 0.92 and a p-value of 0.038. Crystallization end time does not show

a statistically significant correlation, with an R^2 of 0.78 and a *p*-value of 0.78. This is, to a large extent, due to the three center points (marked with green circle), which cannot be mapped by the statistical model.

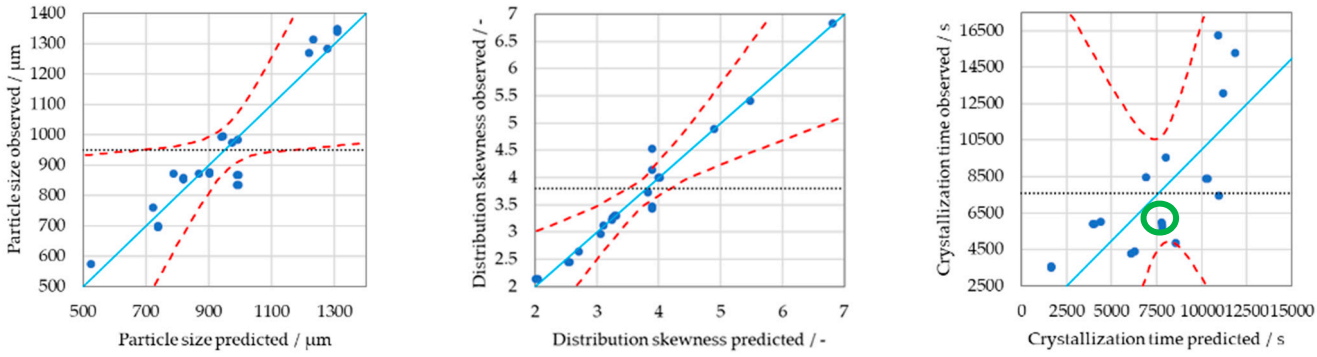

(**a**) (**b**) (**c**)

Figure 4. Results of the linear DoE scheme for (**a**) particle size (x_{63}), (**b**) skewness of the particle size distribution (k), and (**c**) crystallization endtime. The blue line shows ideal fit, the red dashed lines 95% confidence intervals, and the black dashed line the average.

In Table 2, the parameter influence on the skewness of the particle size distribution is given, ranked by the statistical influence on the distribution. Additive volume, for example, correlates most significantly with a more even distribution of particle sizes, the second most important influence is the diameter of the seeding crystals. The largest negative correlation is the interaction of seeding crystal mass and its diameter. The significant influences on the distribution skewness are marked with a star.

Table 2. Parameter influence on the crystal size distribution. The terms marked with a star (*) are statistically significant.

Term	Parameter	Std.-Error	t-Value	Prob > |t|
Additive volume	0.816514	0.122635	6.66	0.0012 *
Diameter seeding crystals (SC)	0.768486	0.122635	6.27	0.0015 *
Mass SC * Diameter SC	−0.76224	0.122635	−6.22	0.0016 *
RPM * additive volume	0.494736	0.122635	4.03	0.0100 *
Mass SC	−0.38546	0.110978	−3.47	0.0178 *
RPM * mass SC	0.345264	0.122635	2.82	0.0373 *
Additive volume * diameter SC	0.317236	0.122635	2.59	0.0490 *
Additive volume * Mass SC	0.089736	0.122635	0.73	0.4972
RPM	−0.07651	0.122635	−0.62	0.56
RPM * diameter SC	−0.02724	0.122635	−0.22	0.833

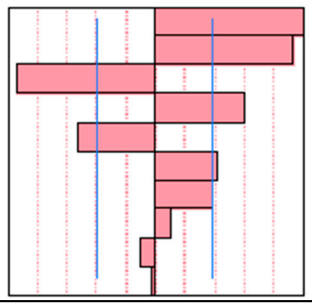

In Table 3, the parameter influence on the crystal size is given. Different parameters correlate to the x_{63} crystal size, when compared to the size distribution. However, the most significant correlation to the crystal size is still the diameter of the seeding crystals as well as the volume of additive. Crystal mass has the largest negative correlation, which can be easily explained, with the higher amount of resulting sugar crystals and, therefore, smaller crystals in general as the supersaturation does not change.

Table 3. Parameter influence on the crystal size (x_{63}). The terms marked with a star (*) are statistically significant.

Term	Parameter	Std.-Error	t-Value	Prob > |t|
Diameter Seeding crystals (SC)	166.9049	37.74014	4.42	0.0069 *
Additive volume * Diameter SC	151.0299	37.74014	4	0.0103 *
Mass SC	−95.2148	34.15285	−2.79	0.0385 *
RPM * Mass SC	−99.2799	37.74014	−2.63	0.0465 *
Additive Volume	81.84507	37.74014	2.17	0.0823
RPM * Diameter SC	76.22007	37.74014	2.02	0.0994
RPM	66.90493	37.74014	1.77	0.1365
Additive volume * Mass SC	−31.7201	37.74014	−0.84	0.4390
Mass SC * Diameter SC	−2.02993	37.74014	−0.05	0.9592
RPM * Additive Volume	1.77993	37.74014	0.05	0.9642

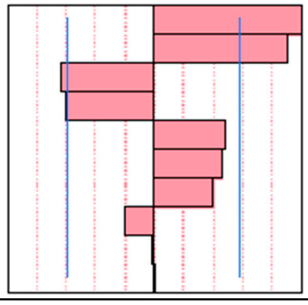

On the evaluation of the DoE, a failure mode and effect analysis (FMEA) can be based, as the impact of failures in the secondary process parameters can be assessed. The resulting FMEA is given in Figure 5. Green influences are the process parameter influences based on the DoE. Occurrence is based on prior knowledge. For example, the additive volume has shown a high impact on the crystallization process, however, in the scale of 1 mL additive per 1 L crystallization volume, it is easily dosed in industrial scales. The grey failures are other possible influences not evaluated in this study which can be expected to have a significant influence, however, solutions to these are already employed in the industrial processes or their occurrence and influence are low. For example, the particle load would have a high relative impact, as it could start the crystallization uncontrollably, this, however, is mitigated by a prior filtration. Supersaturation would have a high impact, however, the occurrence is relatively low, as evaporation is a well-controlled process.

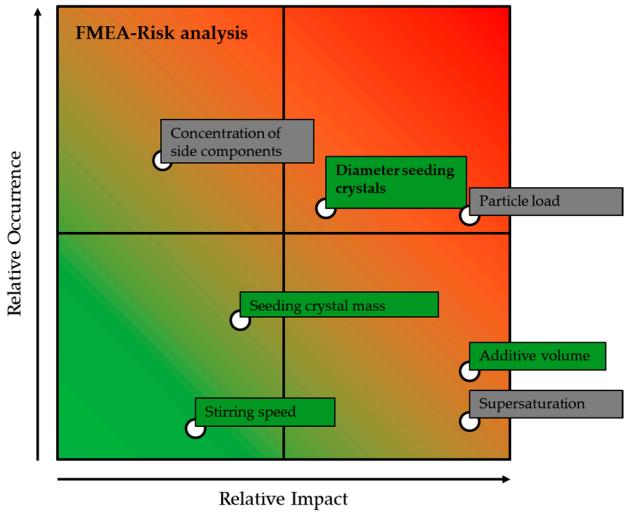

Figure 5. FMEA for the sugar crystallization process.

3.2. Results of the Physico-Chemical Model

Parameter determination was done for the experiments with 0, 1, and 2 mL additive separately, as there is at this point no possibility to model the effects of the additive. The aim of this is to identify the parameters which depend on the additive, whether it changes kinetics, breakage, or agglomeration. In Table 4, the results of the parameter determination are given. For Λ in the center point, the routine returns 0, which is due to the design of the DoE scheme. This parameter scales the influence of stirrer speed on the occurrence of breakage events, and as there was no difference in stirrer speed, the parameter cannot have any influence on breakage, as the breakage events are now reduced to γ according to Equation (14).

Table 4. Results of the parameter determination for the three different additive classes 0, 1, and 2 mL.

Parameter	Value 0 mL	Value 1 mL	Value 2 mL
k_{12}	1.44×10^{-5}	2.34×10^{-6}	7.85×10^{-5}
k_3	1.87	1.11	2.30
γ	7.81×10^{-5}	5.71×10^{-5}	2.40×10^{-5}
Λ	2.25×10^{-3}	0	5.49×10^{-1}
W_{eff}	3.86×10^{-8}	6.61×10^{-1}	5.85×10^{-2}

To evaluate the quality of the determined parameters in Table 5, a statistical evaluation of the training is given. The root-mean square error (RMSE) shows the average error is relatively small, while the result of the overall F-test demonstrates that the effects explained by the model far outweigh the residuals.

Table 5. Statistical evaluation of the determined parameters.

	Value 0 mL	Value 1 mL	Value 2 mL
RMSE	6.746×10^{-2}	3.48×10^{-2}	5.538×10^{-2}
F-test	5.429×10^{4}	1.02×10^{5}	6.581×10^{4}

To visualize these in Figure 6, examples of the parameter estimation are given. The model is able to depict the distribution broadening resulting from changing seed crystals and stirrer speeds. A large extent of the observed errors results from the measurement deviations as can be observed in (b). Here the model would expect a large concentration of crystals in class 3, however, much of the counted crystals are of class 4. In other experiments, as shown in (a), the smaller crystals are overrepresented in the data compared to the model. This is probably due to the smaller crystals are easier to count. Methods to rectify this effect are further discussed in Part 4.

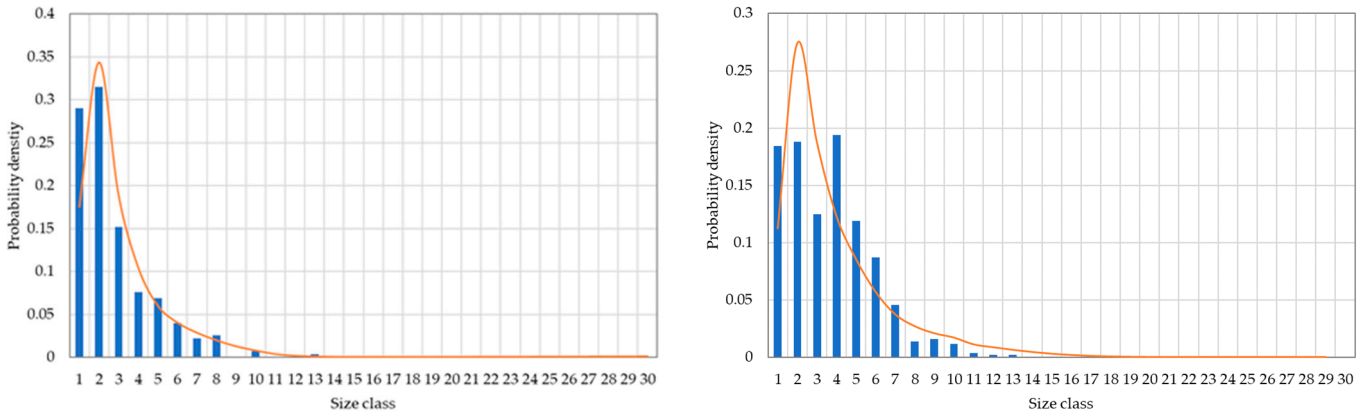

(**a**) (**b**)

Figure 6. Results of the model for two different experiments (**a**,**b**) given as orange lines in comparison to the experiment data, given as blue columns.

The fit of the concentration courses was also satisfying. In Figure 7, the concentration courses of two different experiments are given. Comparing (a) and (b) the range of crystallization times in the DoE, resulting from the secondary effects becomes obvious. The model allows for a good representation of the concentration course, even as the crystallization times change from 5000 to 15,000 s. Experiments shown here are from the 0 mL additive determination scheme, as such, the effects in particle size distribution and crystallization times that can be observed, solely result from the changed initial variables, which are seed crystal mass, size, and stirrer speed.

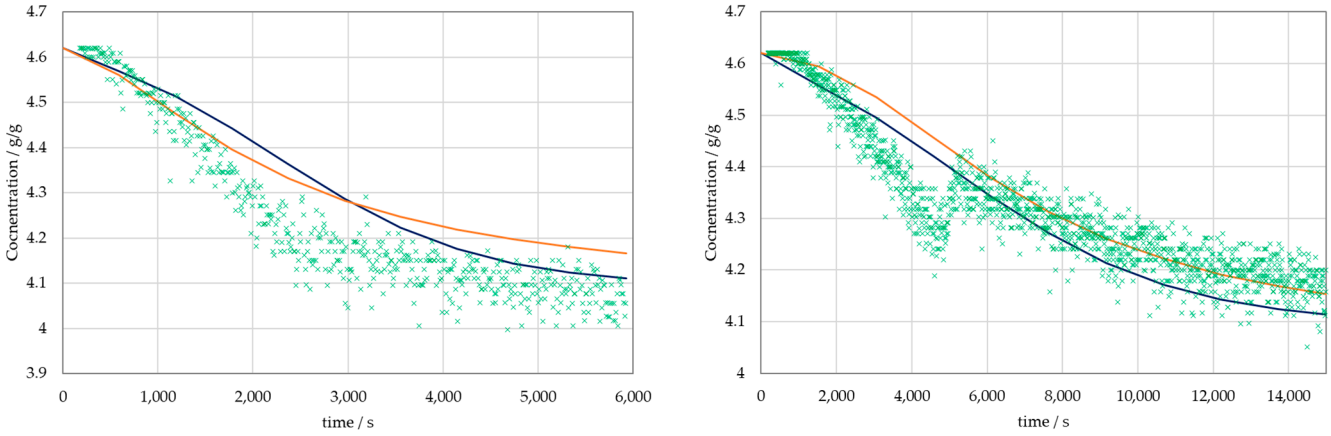

(**a**) (**b**)

Figure 7. The concentration courses for two different experiments (**a**,**b**). Green crosses are measured data, the dark blue line is the sigmoid function fit described in the methods, the orange line is the result of the model.

4. Discussion

Based on the reported data, it is clear that a physico-chemical model holds a significant advantage over a simple statistical evaluation. On the one side, the results of the physico-chemical model are more detailed, especially considering the concentration course, as it not only gives the crystallization end time as a result. On the other hand, the particle size distribution allows for a more complex distribution to take place, i.e., binary density maxima, which is not possible when working with a Weibull probability curve. In addition to these advantages, it should be pointed out that if a validated model is at hand, it can be trained from the same experimental data as the DoE, and therefore does not demand any extra experiments. This is, however, not the case if nucleation should be a factor in the crystallization process [13,16]. Then, polythermal experiments at different stirring rates are needed to evaluate the borders of the metastable area [24]. In this context, it should be noted that the use of primary crystallization and, therefore, nucleation is not widely spread in industrial crystallization due to the resulting challenges for solid–liquid separation [25], which plays a major role in process economics, as described above.

As we set out in the Introduction, the aim of this work is to design a model which can be used to describe the course of an industrial sugar crystallization process given a defined starting point. This enables the model to be used as a predictive tool to alter the starting point and optimize the process outcome. This qualifies the model as a Digital Twin, as opposed to a digital shadow [28]. However, as fluid, mechanically the stirring tank differs significantly from an industrial crystallizer and the parameters have to be adjusted with the help of industrial crystallization data.

The lack of fit of the probability density curves given by the Weibull fit, and to an extent the lack of fit of the physico-chemical model to the experimental data, most probably results from the employed methods to measure the experimental results. The variance of counted crystals for neighboring size classes would call for a higher crystal count to be evaluated. This, however, would be most optimally done dynamically during the crystallization process, as in this way, the data set for parameter determination would be larger and more spread out over the process time and may result in easier model convergence. This data would also enable the ability to better compare a physical and cyber state. As the size distribution is described by the skewness in the DoE, the comparison to the digital twin results is lacking. The simplification of the digital twin results to the Weibull-parameters was not feasible as the lack of fit of the Weibull curve is significant when calculated from the digital twin results. A method to obtain a smoother particle size distribution would be inline, in situ particle size measurements, already employed in wide parts of the industry,

and which effects will be evaluated in future work, allowing us to improve parameter determination and model validation.

Author Contributions: Conceptualization: J.S.; methodology, experimental design, evaluation, and writing: F.L.V.; editing and reviewing: F.L.V. and J.S.; supervision: J.S. All authors have read and agreed to the published version of the manuscript.

Funding: The authors want to gratefully acknowledge the Bundesministerium für Wirtschaft und Energie (BMWi), especially Michael Gahr (Projektträger FZ Jülich), for funding the scientific work. We also kindly acknowledge the support of Open Access Publishing Fund of the Clausthal University of Technology.

Data Availability Statement: Data cannot be made publicly available.

Acknowledgments: The authors would like to thank Sebastian Rettmer, formerly a student at TU Clausthal, for his considerate laboratory work in conducting experiments and microscopic evaluation, as well as the ITVP lab-team, especially Frank Steinhäuser, Volker Strohmeyer, and Thomas Knebel, for their efforts and support.

Conflicts of Interest: The authors declare no conflict of interest. The funders had no role in the design of the study; in the collection, analyses, or interpretation of data; in the writing of the manuscript, or in the decision to publish the results.

References

1. McCabe, W.L.; Smith, J.C.; Harriott, P. *Unit Operations of Chemical Engineering*, 7th ed.; McGraw-Hill Higher Education: Boston, MA, USA, 2005; ISBN 0-07-284823-5.
2. SUSlick, K.S. *Kirk-Othmer Encyclopedia of Chemical Technology*; Wiley: New York, NY, USA, 2013; ISBN 9780471238966.
3. Lambert, C.; Laulan, B.; Decloux, M.; Romdhana, H.; Courtois, F. Simulation of a sugar beet factory using a chemical engineering software (ProSimPlus®) to perform Pinch and exergy analysis. *J. Food Eng.* **2018**, *225*, 1–11. [CrossRef]
4. Mazaeda, R.; Merino, A.; de Prada, C.; Acebes, F. Hybrid modelling of batch centrifuges as part of a generic object oriented beet Sugar Mill library. *Simul. Model. Pract. Theory* **2012**, *22*, 123–145. [CrossRef]
5. Gleiss, M.; Hammerich, S.; Kespe, M.; Nirschl, H. Development of a Dynamic Process Model for the Mechanical Fluid Separation in Decanter Centrifuges. *Chem. Eng. Technol.* **2018**, *41*, 19–26. [CrossRef]
6. Kelly, F.H.C. *Raw Sugar Quality*; Congress of International Society of Sugar Cane Technologists: Durban, South Africa, 1974.
7. Ditz, R.; Gerard, D.; Hagels, H.; Igl, N.; Schäffler, M.; Schulz, H.; Stürtz, M.; Tegtmeier, M.; Treutwein, J.; Strube, J. *Proposal towards a New Comprehensive Research Focus: Position Paper of the ProcessNet-Subject Division Plant Based Extracts—Products and Processes and the European Working Group on Phytoextracts—Products and Processes*; DECHEMA: Frankfurt, Germany, 2017.
8. Huter, M.; Schmidt, A.; Mestmäcker, F.; Sixt, M.; Strube, J. Systematic and Model-Assisted Process Design for the Extraction and Purification of Artemisinin from Artemisia annua L.—Part IV: Crystallization. *Processes* **2018**, *6*, 181. [CrossRef]
9. Both, S.; Eggersglüß, J.; Lehnberger, A.; Schulz, T.; Schulze, T.; Strube, J. Optimizing Established Processes like Sugar Extraction from Sugar Beets—Design of Experiments versus Physicochemical Modeling. *Chem. Eng. Technol.* **2013**, *36*, 2125–2136. [CrossRef]
10. Soares, R.M.; Câmara, M.M.; Feital, T.; Pinto, J.C. Digital Twin for Monitoring of Industrial Multi-Effect Evaporation. *Processes* **2019**, *7*, 537. [CrossRef]
11. Foxon, K.M. An evaporator station model for estimating exhaust steam conversion and consumption. In *ISJ's World Sugar Yearbook*; 2021; pp. 20–31. Available online: https://internationalsugarjournal.com/paper-author/km-foxon/ (accessed on 10 February 2022).
12. Lehnberger, A. IIoT for batch centrifugals—Initial results. In *ISJ's World Sugar Yearbook*; 2021; pp. 86–90. Available online: https://internationalsugarjournal.com/paper/iiot-for-batch-centrifugals-initial-results/ (accessed on 10 February 2022).
13. Mersmann, A.; Braun, B.; Löffelmann, M. Prediction of crystallization coefficients of the population balance. *Chem. Eng. Sci.* **2002**, *57*, 4267–4275. [CrossRef]
14. David, R.; Marchal, P.; Marcant, B. Modelling of agglomeration in industrial crystallization from solution. *Chem. Eng. Technol.* **1995**, *18*, 302–309. [CrossRef]
15. Schmok, K. Modelling of mechanism of agglomeration of KCl crystallization. *Cryst. Res. Technol.* **1988**, *23*, 967–972. [CrossRef]
16. Laloue, N.; Couenne, F.; Le Gorrec, Y.; Kohl, M.; Tanguy, D.; Tayakout-Fayolle, M. Dynamic modeling of a batch crystallization process: A stochastic approach for agglomeration and attrition process. *Chem. Eng. Sci.* **2007**, *62*, 6604–6614. [CrossRef]
17. Codan, L.; Eckstein, C.F.; Mazzotti, M. Growth Kinetics of S—Mandelic Acid in Aqueous Solutions in the Presence of R -Mandelic Acid. *Cryst. Growth Des.* **2013**, *13*, 652–663. [CrossRef]
18. Lucke, M.; Koudous, I.; Sixt, M.; Huter, M.J.; Strube, J. Integrating crystallization with experimental model parameter determination and modeling into conceptual process design for the purification of complex feed mixtures. *Chem. Eng. Res. Des.* **2018**, *133*, 264–280. [CrossRef]

19. Sixt, M.; Uhlenbrock, L.; Strube, J. Toward a Distinct and Quantitative Validation Method for Predictive Process Modelling—On the Example of Solid-Liquid Extraction Processes of Complex Plant Extracts. *Processes* **2018**, *6*, 66. [CrossRef]
20. Kassing, M.; Jenelten, U.; Schenk, J.; Hänsch, R.; Strube, J. Combination of Rigorous and Statistical Modeling for Process Development of Plant-Based Extractions Based on Mass Balances and Biological Aspects. *Chem. Eng. Technol.* **2012**, *35*, 109–132. [CrossRef]
21. Zogg, M. *Einführung in Die Mechanische Verfahrenstechnik: Mit 29 Tabellen und 32 Berechnungsbeispielen*, 3rd ed.; Überarb, A., Ed.; Teubner: Stuttgart, Germany, 1993; ISBN 3-519-16319-5.
22. Stieß, M. *Verfahrenstechnik in Beispielen*; Draxler, J., Siebenhofer, M., Eds.; Springer Fachmedien Wiesbaden: Wiesbaden, Germany, 2014; ISBN 978-3-658-02739-1.
23. Uhlenbrock, L.; Jensch, C.; Tegtmeier, M.; Strube, J. Digital Twin for Extraction Process Design and Operation. *Processes* **2020**, *8*, 866. [CrossRef]
24. Huter, M. Modellunterstützte Prozessauslegung Unterschiedlicher Grundoperationen am Beispiel von Kontinuierlicher Ultrafiltration und Absatzweiser Kristallisation. Ph.D. Dissertation, Technische Universität Clausthal, Clausthal-Zellerfeld, Germany, November 2020.
25. Hofmann, G. *Kristallisation in der Industriellen Praxis*; Wiley-VCH: Hoboken, NJ, USA, 2007; ISBN 9783527608881.
26. Schuchmann, H.; Szembek, M.; Grüneberg, M.; Schubert, H. Einfluss von Partikeleigenschaften und Prozessparameter auf das Strahlagglomerieren von Getränkepulvern. *LWT Food Sci. Technol.* **1994**, *27*, 350–357. [CrossRef]
27. Ramkrishna, D. *Population Balances: Theory and Applications to Particulate Systems in Engineering*; Academic Press: San Diego, CA, USA, 2000; ISBN 978-0-12-576970-9.
28. Bergs, T.; Gierlings, S.; Auerbach, T.; Klink, A.; Schraknepper, D.; Augspurger, T. The Concept of Digital Twin and Digital Shadow in Manufacturing. *Procedia CIRP* **2021**, *101*, 81–84. [CrossRef]